European Radiology (2019) 29:5013–5021
https://doi.org/10.1007/s00330-018-5996-8

INTERVENTIONAL

Can we ablate liver lesions close to large portal and hepatic veins with MR-guided HIFU? An experimental study in a porcine model

Ulrik Carling[1,2] · Leonid Barkhatov[2,3,4] · Henrik M. Reims[5] · Tryggve Storås[4] · Frederic Courivaud[4] · Airazat M. Kazaryan[4,6,7,8] · Per Steinar Halvorsen[4] · Eric Dorenberg[1] · Bjørn Edwin[2,4,9] · Per Kristian Hol[2,4]

Received: 8 June 2018 / Revised: 20 August 2018 / Accepted: 28 December 2018 / Published online: 8 February 2019

Abstract

Objectives Invasive treatment of tumors adjacent to large hepatic vessels is a continuous clinical challenge. The primary aim of this study was to examine the feasibility of ablating liver tissue adjacent to large hepatic and portal veins with magnetic resonance imaging–guided high-intensity focused ultrasound (MRgHIFU). The secondary aim was to compare sonication data for ablations performed adjacent to hepatic veins (HV) versus portal veins (PV).

Materials and methods MRgHIFU ablations were performed in six male land swine under general anesthesia. Ablation cells of either 4 or 8 mm diameter were planned in clusters (two/animal) adjacent either to HV ($n = 6$) or to PV ($n = 6$), with diameter ≥ 5 mm. Ablations were made using 200 W and 1.2 MHz. Post-procedure evaluation was made on contrast-enhanced MRI (T1w CE-MRI), histopathology, and ablation data from the HIFU system.

Results A total of 153 ablations in 81 cells and 12 clusters were performed. There were visible lesions with non-perfused volumes in all animals on T1w CE-MRI images. Histopathology showed hemorrhage and necrosis in all 12 clusters, with a median shortest distance to vessel wall of 0.4 mm (range 0–2.7 mm). Edema and endothelial swelling were observed without vessel wall rupture. In 8-mm ablations ($n = 125$), heat sink was detected more often for HV (43%) than for PV (19%; $p = 0.04$).

Conclusions Ablations yielding coagulative necrosis of liver tissue can be performed adjacent to large hepatic vessels while keeping the vessel walls intact. This indicates that perivascular tumor ablation in the liver is feasible using MRgHIFU.

Key Points

- *High-intensity focused ultrasound ablation is a non-invasive treatment modality that can be used for treatment of liver tumors.*
- *This study shows that ablations of liver tissue can be performed adjacent to large hepatic vessels in an experimental setting.*
- *Liver tumors close to large vessels can potentially be treated using this modality.*

Keywords High-intensity focused ultrasound ablation · Interventional magnetic resonance imaging · Liver · Portal veins · Hepatic veins

Abbreviations

BW	Bandwidth
CEUS	Contrast-enhanced ultrasound
DT	Dynamic scan time
EM	Equivalent minutes
FA	Flip angle

✉ Ulrik Carling
johcar@ous-hf.no

[1] Department of Radiology and Nuclear Medicine, Oslo University Hospital, Post box 4950, N-0424 Oslo, Norway

[2] Institute of Clinical Medicine, University of Oslo, Oslo, Norway

[3] Department of Gastrointestinal Surgery, Haukeland University Hospital, Bergen, Norway

[4] The Intervention Center, Oslo University Hospital, Oslo, Norway

[5] Department of Pathology, Oslo University Hospital, Oslo, Norway

[6] Department of Surgery, Fonna Hospital Trust, Stord, Norway

[7] Department of Surgery No. 1, Yerevan State Medical University after M. Heratsi, Yerevan, Armenia

[8] Department of Faculty Surgery No. 2, I.M. Sechenov First Moscow State Medical University, Moscow, Russia

[9] Department of Hepato-Pancreato-Biliary Surgery, Oslo University Hospital, Oslo, Norway

FFE	Fast field echo
GRE-EPI	Gradient echo sequence with echo-planar readout
HCC	Hepatocellular carcinoma
HIFU	High-intensity focused ultrasound
MRgHIFU	Magnetic resonance imaging–guided high-intensity focused ultrasound
NPV	Non-perfused volume
PFS	Proton frequency shift
PS	Pixel sum
SENSE	Sensitivity encoding
SpO_2%	Oxygen saturation
T1w	T1 weighted
T2w	T2 weighted
TE	Echo time
TFE	Turbo field echo
TR	Repetition time
USgHIFU	Ultrasound-guided high-intensity focused ultrasound
VS	Voxel size

Introduction

Treatment of liver tumors is often multimodal, where surgery and liver transplantation are the gold standards for curative treatment in patients where these techniques are amendable [1–3]. Tumors located close to central and large portal and hepatic veins are often difficult to remove surgically, requiring extensive surgery or making the patient inoperable [4–6]. As many patients cannot have surgery, thermal ablative techniques such as radiofrequency and microwave ablation are important treatment alternatives [7, 8]. These invasive techniques depend on heat conduction and are sensitive to heat loss close to vessels, the heat sink effect, which might influence treatment outcome adjacent to large portal and hepatic veins [9, 10].

High-intensity focused ultrasound (HIFU) is a non-invasive ablation modality in which the energy in ultrasound waves is used to produce heat in a desired focal spot. HIFU can ablate sharply delineated volumes [11] and is potentially less sensitive to heat sink than ablative methods depending on heat conduction. HIFU may be performed either under ultrasound guidance (USgHIFU) or under magnetic resonance (MR) guidance [12, 13]. Both systems have advantages and disadvantages [14], but only MR-guided HIFU (MRgHIFU) offers the possibility for thermal control during the treatment by the use of temperature-sensitive MR sequences [15]. This technique offers an improved control of the ablation where the HIFU system gives fast feedback regarding targeting and potential heat sink, which is particularly important during perivascular liver ablation. Zhang et al [16] published treatment outcomes after USgHIFU close to (< 10 mm) large hepatic veins in patients with hepatocellular carcinoma (HCC) and described complete tumor necrosis without vessel damage on follow-up imaging. However, the study did not report histopathological assessment of the ablated area. Jiang et al [17] examined the effect of portal veins on small MRgHIFU ablations in goat liver and described that the distance to the portal veins influenced the energy needed to perform an ablation. They also described histopathological vessel damage on ablations aimed at the vessel wall. Another study on porcine liver has indicated that HIFU ablation can be performed adjacent to vessels above 4 mm of size without vessel damage [18]. Despite these efforts, there is still scanty knowledge regarding MRgHIFU ablations of clinically relevant volumes close to large hepatic and portal veins.

The aim of the present study was to examine the feasibility of ablating normal liver tissue adjacent to large portal and hepatic veins while keeping the vessel wall intact. The secondary aim was to compare sonication data for ablations adjacent to hepatic versus portal veins.

Material and methods

Animals and anesthesia protocol

The study was approved by the National Animal Research Authority (project no. 67/13-5340.). Seven male land swine with a median weight of 21.5 kg (range 18–28.5 kg) were used in an acute study protocol. Anesthesia was induced by intramuscular ketamine (20 mg/kg), azaperone (3 mg/kg), and atropine (20 μg/kg). Anesthesia was maintained intravenously including pentobarbital (4 mg/kg/h), morphine (2 mg/kg/h), midazolam (0.15 mg/kg/h), and rocuronium bromide (3 mg/kg/h) for all but the first animal, in which gas anesthesia with isoflurane and morphine was used. Tracheostomy, jugular venous and carotid arterial accesses, and a gastric tube were placed in all animals. MRI compatible surveillance equipment was used for monitoring heart rate, central venous pressure, exhale CO_2 concentration, SpO_2%, and body temperature during the procedures. Median anesthesia time was 635 (range 520–720) min. The pigs were euthanized after final imaging with intravenous injections of pentobarbital (20 mg/kg), morphine (1 mg/kg), and potassium chloride (1 mmol/kg). One animal (animal 4) had cardiac arrest before ablation was initiated and was excluded from the study.

Imaging protocol

The position of the liver was determined by diagnostic ultrasound, and the optimal HIFU transducer position was marked on the skin after shaving. The animals were placed on the MRI table in the prone position with the right upper quadrant facing the in-table HIFU transducer, in accordance with the applied skin marks. A gel pad was placed between the HIFU transducer and the skin. An overview of the setup is displayed in Fig. 1.

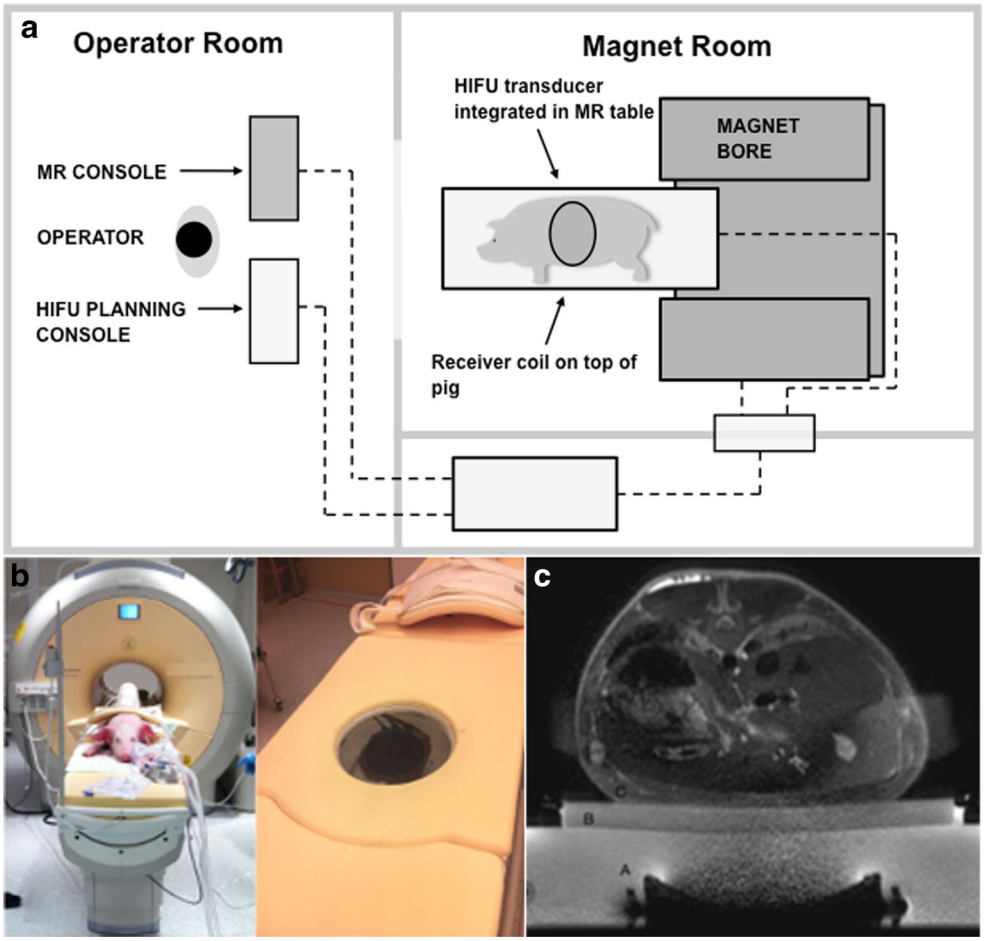

Fig. 1 Procedure setup for the MR-guided HIFU ablation. **a** Overview of the MRgHIFU experiment setup. The MR and the HIFU systems are connected, and this setup allows for the HIFU system to control the MR system during the ablations. MR images can be obtained during planning, for treatment monitoring (temperature measurements), and for post treatment evaluation. **b** The HIFU transducer is integrated in the MR table (right), and the receiver coil is placed on top of the pig (left). **c** Axial T2-weighted MR image showing the HIFU transducer in degassed water (A), a gel pad (B), and the pig in a prone position (C) with the liver facing the HIFU transducer

Imaging was performed in breath-hold in exhale. MR images were acquired using a 3.0-T MRI system (Achieva, Philips, software release 2.6.3), equipped with an integrated HIFU transducer, with a three-channel receiver coil (one coil element around the HIFU transducer integrated in the table top and a two-channel flex coil element placed on the back of the animals). Pre-sonication sequences included a sequence to detect air bubbles at the skin surface in the anticipated HIFU beam path (Table 1: sequence 1). For all animals, a T1-weighted (T1w) sequence for vessel detection and visualization of potential beam obstructions (e.g., ribs) was performed (Table 1: sequence 2). This sequence was repeated during the procedures to avoid unintentional shift of focus due to movement.

During sonication, and until 30 s after, proton frequency shift (PFS) temperature maps were generated (Table 1: sequence 3). Temperature measurements were generated with three coronal slices and one sagittal slice at the HIFU focus position. Measurements were also performed with one coronal slice in the near field and one in the far field. Temperature curves were generated automatically, and maximum temperature and time to maximum temperature (ΔT) were assessed from these curves.

Contrast-enhanced T1w (T1w CE-MRI) images (Table 1: sequence 4) were acquired with gadolinium contrast (0.1 mmol/kg, Dotarem, Guerbet Laboratories Ltd). The non-enhancing volume at the ablation site was defined as non-perfused volume (NPV) and measured in three planes on T1w CE-MRI as an expression for the size of the ablated lesion.

Following the MRI studies, contrast-enhanced ultrasound (CEUS) was performed in animals 2–7, using 1.25 ml sulfur hexafluoride (8 μl/ml, Sonovue, Bracco Imaging), to further study the patency of the vessels adjacent to the ablation zones.

HIFU protocol

The HIFU system (Sonalleve, Profound Medical), including a 256-channel transducer, was controlled through software designed for clinical uterine fibroid ablation (release R2.1 L2).

In each animal, two separate intrahepatic vessels reachable by the HIFU beam were identified on the T1w images. The targeted vessels were either hepatic veins ($n = 6$; size 7 mm; *range 6–8 mm*) or portal veins ($n = 6$; size 7 mm; *range 5–12 mm*). Additional adjacent vessels were defined as secondary vessels. Separate clusters, two in each animal, consisting of 8-mm volumetric sonication cells were placed adjacent to the target vessels (Fig. 2). The 8-mm cells were 20 mm in length, with a maximum volume of 0.7 ml per cell. The cells

Table 1 MRI sequences used for HIFU ablation planning, temperature measurements, and post-ablation evaluation

Sequence	Sequence description
1. Air bubble detection at skin surface	Coronal 3D time reversed T2 FFE[1]
	TR[2]/TE[3] = 10/13 ms
	FA[4] = 10°
	VS[5] = 1.09 × 1.10 × 2.0 mm^3
	BW[6] = 542.5 Hz/pixel
	Acquisition time = 72 s*
	Matrix size = 256 × 256
2. Ablation planning	Sagittal 3D T1 FFE
	TR/TE = 2.7/1.2 ms
	FA = 7°
	VS = 1.25 × 1.5 × 2.5 mm^3
	SENSE[7] factor 1.5
	BW = 864.6 Hz/pixel
	Acquisition time = 90 s*
	Matrix size = 192 × 160
3. Thermometry	Fat-saturated GRE-EPI[8]
	TR/TE = 47/19.5 ms
	FA = 19.5°
	VS = 2.5 × 2.5 × 7.0 mm^3
	BW = 79 Hz/pixel
	DT[9] = 4.2 s
	Matrix size = 160 × 99
4. Post-ablation evaluation	Transverse 3D fat suppressed T1 TFE[10]
	TR/TE = 3.0/1.34 ms
	FA = 10°
	VS = 1.99 × 2.02 × 4.0 mm^3
	SENSE factor 1.5, BW = 721.6 Hz
	3D volume DT = 20 s
	Acquisition time = 114 s*
	Matrix size = 188 × 186

[1] *FFE* fast field echo, [2] *TR* repetition time, [3] *TE* echo time, [4] *FA* flip angle, [5] *VS* voxel size, [6] *BW* bandwidth, [7] *SENSE* sensitivity encoding, [8] *GRE-EPI* gradient echo with echo-planar readout, [9] *DT* dynamic scan time, [10] *TFE* turbo field echo

*Total acquisition time for the diagnostic sequences 1, 2, and 4 was approximately 4.5 min

were placed partly in the targeted vessel, and the volume covered by the ablation, but excluding the vessel, was defined as planned volume. The planned volume was assessed by manual measurements on the pre-ablation MRI images, assuming ellipsoid shape. Clusters included 5–7 sonication cells in all animals but in pig 5, in which also 4-mm cells (1 cm of length; 28 cells adjacent to two separate hepatic veins) were used due to near-field heating.

Following test sonications with 30–60 W of acoustic power, treatment sonications with a power of 200 W and a frequency of 1.2 MHz were performed. Treatment sonications were performed twice in each cell to ensure necrosis [11], and cells within a cluster were sonicated in such an order that adjacent cells were not sonicated directly after each other. Each sonication cycle was performed during 1 minute breath-hold in exhale and included 27.5 s (range *5.2–27.8*) of sonication followed by post-sonication temperature monitoring. Following the sonication, the HIFU system gives an estimated cooling time to allow for tissue cooling before the next ablation is considered safe.

The ablated volume was given automatically by the HIFU system based on thermal dose with 240 equivalent minutes (EM) and 30 EM separately, as reported by Sapareto et al [19]. In addition, the volume was calculated from manual measurements on the temperature maps, assuming ellipsoid shape. Further, the number of pixels with 240 EM was calculated in the temperature maps and summarized, and defined as pixel sum. For each sonication the planned treatment cell was compared with the actual area of registered thermal dose on the temperature maps, and any difference in position was recorded as an offset in millimeter (mm).

Histopathological protocol

The livers were promptly removed and put in 10% formalin following euthanasia. The livers were sliced perpendicular to the anticipated HIFU beam path. The tissue of interest adjacent to the targeted vessels was removed and cut in approximately 3-mm slices, which were processed according to a routine protocol and embedded in paraffin wax. Histological sections from each sample were stained with hematoxylin and eosin and examined by light microscopy by a pathologist (HMR) with experience in hepatic histopathology. The histopathological examination focused on assessing necrosis and hemorrhage related to the ablation zone and included type of vein, distance between vessel and ablation zone, and presence of vein damage.

Statistical analyses

For comparisons between portal and hepatic veins, only cells with 8-mm ablations were included. For this purpose, generalized linear mixed models were built with vein type (portal vs. hepatic) as fixed effect and lesion number as random effect with the variables of interest as targets. Logistic regression models (using a binomial distribution with logit link) were fitted for binary target variables, and gamma regression models (using a gamma distribution with log link) were fitted for right-skewed continuous variables. The logistic mixed model for heat sink was then extended to a multivariable model by including planned volume and secondary vessel as additional fixed effects. All analyses were performed with IBM SPSS 25.0 (IBM Corporation). A p value < 0.05 was considered statistically significant.

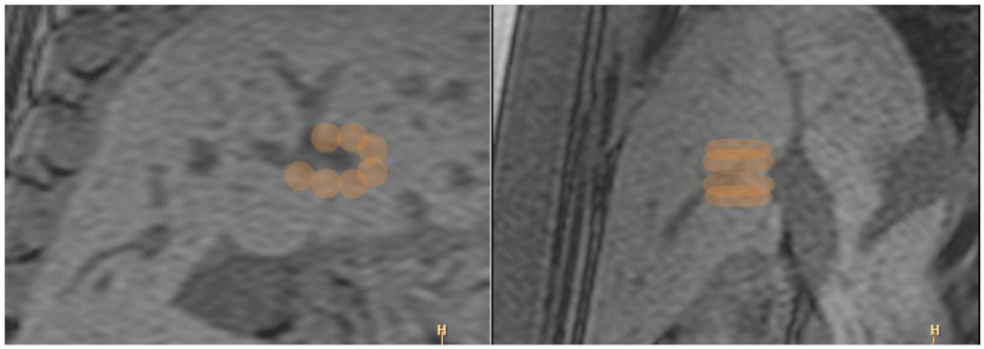

Fig. 2 Example of planning of ablation cells adjacent to a portal vein. T1-weighted MRI images with planned ablation cells (yellow) of 8 mm in diameter adjacent to a portal vein (dark); coronal view to the left and sagittal view to the right (pig 7). The cells are placed with parts of them including the vessel wall and lumen. Each cell was ablated twice using 200 W and 1.2 MHz

Results

A total of 153 ablations were performed in 81 cells, in a total of 12 lesions, two lesions per animal. Of these, 125 were performed in 8-mm cells, and 28 in 4-mm cells. A total of 79 ablations were aimed at hepatic veins and 74 ablations were aimed at portal veins. The HIFU software recorded displacement in 59 (39%) ablations. For the 8-mm cells, the median offset was 4.1 mm (range *0–20*). Insufficient heating was recorded in 50 (33%) ablations, and 26 (17%) had pixel sum of 0–1.

On post-ablation MRI imaging, there were visible lesions with NPV (Fig. 3) in all animals on T1w CE-MRI images corresponding to the planning on pre-ablation images, although three lesions were relatively small (Table 2). The vessels adjacent to these three lesions were unaffected based on imaging, whereas in the rest of the lesions, the adjacent vein had reduced diameter due to compression. In one case, vein occlusion was suspected on MRI and verified on CEUS, whereas CEUS verified patency in two other cases with heavily compressed veins. These three cases were all portal veins (Table 2).

The histopathological analysis of the 12 lesions revealed hemorrhage and necrosis in all lesions. The median shortest distance to the outer margin of the vessel wall was 0.4 mm (range 0–2.7 mm). Edema around the vessel was seen in almost all the cases, and in some cases, also endothelial changes as well as alterations in vessel wall smooth muscle cells were observed (Table 3). Microscopic images are shown in Fig. 4.

Regarding comparison of ablations aimed at portal or hepatic veins, an overview for the 8-mm cells ($n = 125$) is summarized in Table 4. Heat sink was detected by the HIFU system more often in ablations aimed at hepatic veins ($p = 0.045$). More of the ablations adjacent to liver veins were close to a secondary vessel

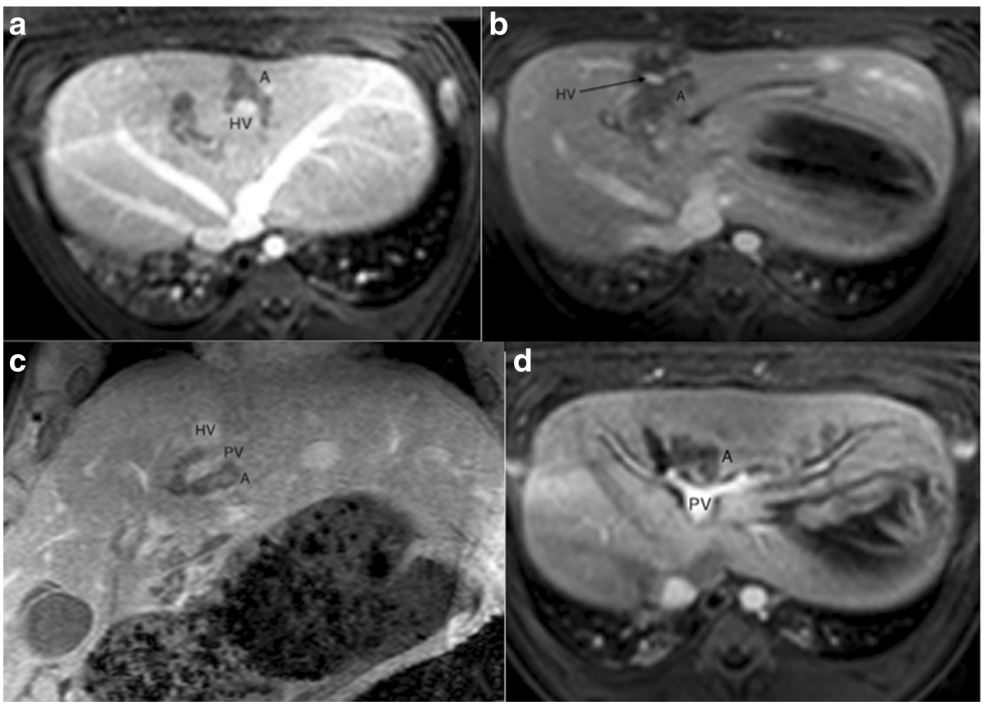

Fig. 3 Post-ablation MR imaging. Contrast-enhanced T1-weighted images showing an area of non-perfused tissue post-ablation (dark, A) adjacent to vein (bright; PV portal vein, HV hepatic vein). **a** Axial view (pig 2). Ablation performed adjacent to a hepatic vein. **b** Axial view (pig 3). Ablation performed adjacent to a hepatic vein. The apparent discontinuity of the vessel is due to the angulation of the vessel. **c** Coronal view (pig 3). Ablation performed adjacent to a portal vein. **d** Axial view (pig 7). Ablation performed adjacent to a portal vein. A portal vein branch was near occluded

Table 2 Description of vessels aimed at during HIFU ablations, and post-ablation findings on T1w contrast-enhanced MRI

Lesion	Vessel[1]	Vessel size (mm)	Ablation size[2] (w l h mm)	Vessel imaging
Pig 1 lesion 1	PV	6	19 × 24 × 23	Compressed[3], open
Pig 1 lesion 2	PV	5	18 × 16 × 21	Compressed, open
Pig 2 lesion 1	HV	7	19 × 33 × 28	Compressed, open
Pig 2 lesion 2	PV	7	31 × 30 × 28	Compressed, occluded*
Pig 3 lesion 1	HV	7	25 × 39 × 18	Compressed, open
Pig 3 lesion 2	PV	5	22 × 33 × 20	Compressed, open*
Pig 5 lesion 1	HV	6	21 × 30 × 20	Compressed, open
Pig 5 lesion 2	HV	6	18 × 20 × 23	Compressed, open
Pig 6 lesion 1	PV	12	9 × 11 × 13	No sure affection
Pig 6 lesion 2	HV	8	6 × 15 × 12	No sure affection
Pig 7 lesion 1	HV	8	8 × 28 × 11	No sure affection
Pig 7 lesion 2	PV	10	22 × 22 × 24	Compressed, open*

[1] Portal vein (PV) and hepatic vein (HV)

[2] Largest measurement of non-perfused volume including targeted vessel on contrast-enhanced T1w MRI

[3] Reduction of vessel size in relation to the ablated lesion

*Evaluation aided by contrast-enhanced ultrasound

(all portal vein branches; 34 vs. 10, $p = 0.001$). Further, more of the planned ablations adjacent to hepatic veins included the vessel compared to portal veins, and hence, the planned volume was smaller ($p = 0.005$). A logistic regression on heat sink showed a significant ($p = 0.03$) odds ratio of 15.0 for heat sink in ablations adjacent to hepatic veins (Table 5).

Discussion

This study confirms the feasibility of ablating clinically relevant volumes of liver tissue close both to hepatic and portal veins, using a commercially available MRgHIFU system.

Histopathological examinations confirmed ablated liver tissue close to the vessels (median 0.4 mm), with relatively mild changes in the vessel walls. In an experimental study, Jiang et al [17] described several small "fractures" and collagen swelling in the vessel walls, however with limited findings 1 week after the ablations. Cases of vessel occlusion/near occlusion (as seen on MRI and CEUS) in our study were all portal vein branches. Similar findings have been described for radiofrequency and microwave ablation [10, 20]. The clinical implications of such occlusions seem to be of minor importance [21], but further attention is needed. We did not evaluate smaller vessels (< 5 mm) due to the fact that vessels below 5 mm are more sensitive to thermal ablation as they generate less heat sink [10, 18], and are more prone to thrombosis. Tumor vascularity also plays

Table 3 Histopathological findings following HIFU ablation

Lesion	Vessel[1]	Distance[2]	Interv. tissue[3]	Liver damage	Vein wall damage
Pig 1 lesion 1	PV	1.00	CT	1, 2	3
Pig 1 lesion 2	PV	0.00	No	1, 2	1, 3, 4
Pig 2 lesion 1	HV	0.00	No	1, 2	1, 3, 4
Pig 2 lesion 2	PV	1.30	CT	1, 2	4
Pig 3 lesion 1	HV	0.00	No	1, 2	1, 3, 6
Pig 3 lesion 2	PV	0.00	No	1, 2	4, 5
Pig 5 lesion 1	HV	0.10	Liver	1, 2	4
Pig 5 lesion 2	HV	0.10	Liver	1, 2	4, 5
Pig 6 lesion 1	PV	2.70	Liver + CT	1, 2	4
Pig 6 lesion 2	HV	1.80	Liver	1, 2	4, 5
Pig 7 lesion 1	HV	0.70	Liver	1, 2	4, 5
Pig 7 lesion 2	PV	2.40	Liver + CT	1, 2	3

1 = hemorrhage, 2 = necrosis, 3 = endothelial changes/swelling, 4 = edema, 5 = smooth muscle damage, 6 = detachment of vein wall from liver tissue—considered to represent artifact

[1] Portal vein (PV) and hepatic vein (HV)

[2] Distance between vessel wall and ablation measured in mm

[3] Intervening tissue between vessel and ablation—connective tissue (CT) and liver parenchyma

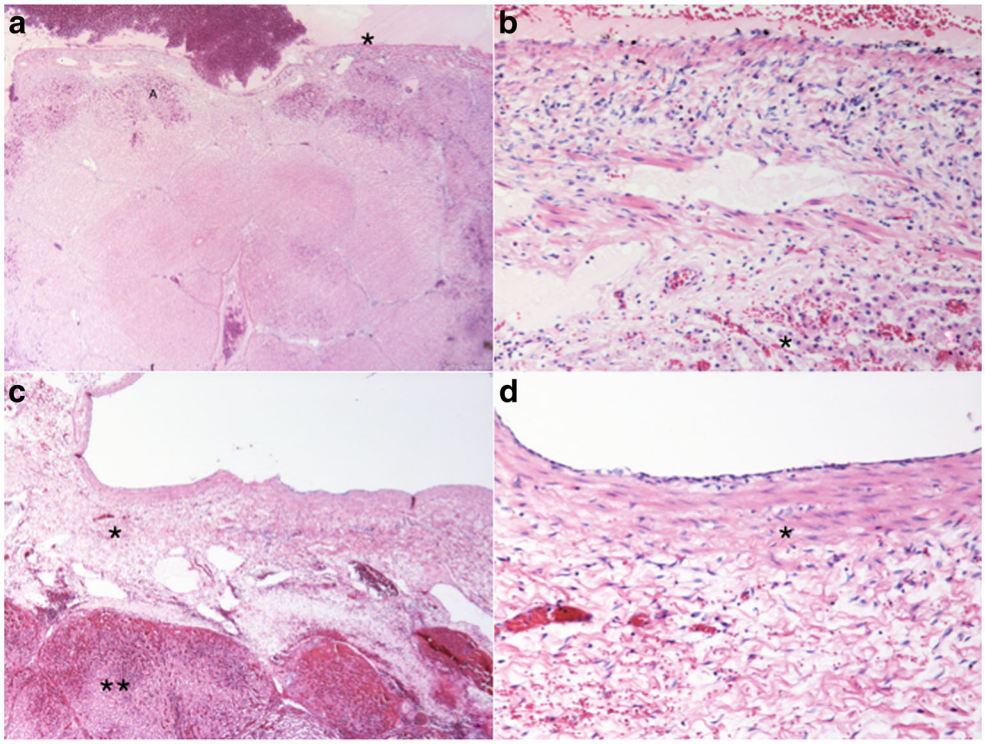

Fig. 4 Microscopic histopathology images after hematoxylin and eosin staining of ablations adjacent to hepatic and portal veins. **a** Ablation adjacent to hepatic vein in pig 2. Magnification × 20. Top (*): vessel lumen and wall. Ablation involves the dominating part of the picture. A = hemorrhagic liver parenchyma in periphery of ablation zone. **b** Ablation adjacent to hepatic vein in pig 2. Magnification × 200. Top and middle: vessel wall with smooth muscle changes and edema. Bottom (*): hemorrhagic liver parenchyma in periphery of ablation zone (A in **a**). **c** Ablation adjacent to portal vein in pig 7. Magnification × 40. Center and left (*): vessel wall. Bottom (**): hemorrhagic liver parenchyma in periphery of ablation zone, similar to A in **a**. **d** Ablation adjacent to portal vein in pig 7. Magnification × 200. Top half (*) shows intact smooth muscle in vessel wall. Bottom half shows edema and hemorrhage in surrounding connective tissue

Table 4 Results of 8-mm HIFU ablations with respect to the type of vessel

	Portal vein ($n = 74$)	Hepatic vein ($n = 51$)	Total ($n = 125$)	p value
Planned vol.[1] (ml*)	0.33 (0.06–0.70)	0.25 (0.02–0.57)	–	0.005
Heat sink	14 (18.9%)	22 (43.1%)	36 (28.8%)	0.043
Max temp (°C)	66.4 (48.5–87.1)	71.8 (50.1–95.1)	–	0.314
Cooling time (s)	147 (90–1738)	231 (90–1787)	–	0.860
ΔT^2	1.16 (0.29–2.74)	0.77 (0.36–3.46)	–	0.522
Pixel sum[3]	25.5 (0–91)	11 (0–65)	14 pixels (0–32)	0.771
Volume S[4] (ml)	0.41 (0–2.5)	0.16 (0–1.77)	0.25 ml (0–2.50)	0.343
Volume M[5] (ml)	0.53 (0–2.26)	0.20 (0–1.89)	0.38 ml (0–2.26)	0.969
Displace reg.[6] y/n	28 (37.8%)	20 (39.2%)	48 (38.4%)	0.240
Offset[7]	4.0 (0–14.5)	4.7 (0–20)	4.1 (0–2.0)	0.116
Sec. vessel y/n[8]	10	34	–	0.001

*Median (range)

[1] Volume of ablation not including vessel

[2] Temperature change per second

[3] Sum of ablated pixels on temperature maps

[4] Ablated volume given by software

[5] Ablated volume manually measured on temperature maps

[6] Automatically registered displacement by software

[7] Distance between planned and detected focal spots as measured on temperature maps

[8] Ablation additionally close to another vessel (3–10 mm of size)

Table 5 Logistic regression on heat sink

	Odds ratio	*p* value
Vessel type (hepatic vs. portal vein)	15.0	0.033
Secondary vessel[1]	1.0	0.99
Planned volume[2]	0.11	0.28

[1] Adjacent non-target vessel (3–10 mm of size)

[2] Planned volume of ablation not including the vessel

a significant role in the clinical setting [22]. Hence, verification of our findings in clinical tumor ablation is important.

Although 200 W (the maximum power allowed by the HIFU system) was used, there were ablations not yielding enough energy to reach ablative temperature. Also, target displacement was registered in more than one third of the 8-mm ablations with a median offset of 4 mm. The use of a more liver-dedicated protocol with increased acoustic power and smaller cells as described by Wijlemans et al [23] might overcome these issues. In addition, alternative ablative strategies such as use of shockwaves [24] or intentional cavitation [25] might be alternate methods of overcoming heat sink issues. However, cavitation can be unpredictable [11], and how to control cavitation in ablations close to large vessels has, to our knowledge, not been investigated.

Several limitations to the study should be noted. Heat sink was detected more often around hepatic veins as compared with that around portal veins. This finding should be interpreted with care due to the overall small number of animals. An optimal protocol for evaluating differences between hepatic and portal veins would have included more animals in which ablations were performed adjacent to many separate target vessels, rather than clusters of ablations performed adjacent to one target vessel. Also, there were differences in the two vessel groups in planned volume and in number of ablations affected by a nearby secondary vessel, and this can potentially have influenced the observed difference in heat sink. However, vessel type (hepatic vein) did have a significant odds ratio for heat sink in regression analysis, which is also supported by the findings of near-/occluded portal vein branches. To our knowledge, there have been no studies comparing MRgHIFU adjacent to hepatic and portal veins. However, our findings are supported by an experimental study in pigs ablated with microwave ablation by Chiang et al [20], as well as by a recent clinical study in HCC patients [21]. An explanation for the disparity in heat sink might be differences in blood flow in hepatic veins and portal veins [21, 26, 27], as well as differences in thickness and composition of the vessel walls [28], facilitating more heat sink adjacent to hepatic veins. In contrast, there are also studies on microwave ablation describing relatively more heat sink close to portal veins, hence contradicting our finding [29, 30]. This indicates a need for further studies on MRgHIFU ablation close to hepatic and portal veins.

This study is experimental and findings are not directly applicable to clinical tumor ablation in humans. The fundamental model is artificial as tumors in the liver do not usually grow circumferential to vessels, but rather one side of the tumor is close to a vessel [9]. Further, we did not assess safety regarding near- or far-field heating, which limits the translation of the findings to the clinical setting. Other limitations include that only one power level (200 W) was used and that we did not assess the effect on and of vessels smaller than 5 mm.

In conclusion, this study demonstrates the feasibility of ablating clinically relevant volumes of liver tissue close to large hepatic and portal veins using MRgHIFU. Ablations can be made close to the vessel without vessel wall rupture, although occlusion can occur especially when ablating adjacent to portal veins. The heat sink effect seems to be more prone adjacent to hepatic veins than adjacent to portal veins.

Funding This study has received funding by The Norwegian Cancer Society (Kreftforeningen).

Compliance with ethical standards

Guarantor The scientific guarantor of this publication is Per Kristian Hol Prof. M.D., The Intervention Center, Oslo University Hospital and Institute of Clinical Medicine, University of Oslo.

Conflict of interest The authors of this manuscript declare no relationships with any companies, whose products or services may be related to the subject matter of the article.

Statistics and biometry Manuela Zucknick, Oslo Centre for Biostatistics and Epidemiology, Faculty of Medicine, Oslo University, kindly provided statistical advice for this manuscript.

Ethical approval Approval from the Institutional Animal Care Committee was obtained.

Methodology
• experimental

References

1. Frankel TL, D'Angelica MI (2014) Hepatic resection for colorectal metastases. J Surg Oncol 109:2–7
2. European Association For The Study Of The Liver; European Organisation For Research And Treatment Of Cancer (2012) EASL-EORTC clinical practice guidelines: management of hepatocellular carcinoma. J Hepatol 56:908–943
3. Van Cutsem E, Cervantes A, Nordlinger B, Arnold D, ESMO Guidelines Working Group (2014) Metastatic colorectal cancer: ESMO Clinical Practice Guidelines for diagnosis, treatment and follow-up. Ann Oncol 25(Suppl 3):iii1–iii9

4. Xiao Y, Li W, Wan H, Tan Y, Wu H (2018) Central hepatectomy versus major hepatectomy for patients with centrally located hepatocellular carcinoma: a meta-analysis. Int J Surg 52:297–302
5. Yu WB, Rao A, Vu V, Xu L, Rao JY, Wu JX (2017) Management of centrally located hepatocellular carcinoma: update 2016. World J Hepatol 9:627–634
6. Azoulay D, Pascal G, Salloum C, Adam R, Castaing D, Tranecol N (2013) Vascular reconstruction combined with liver resection for malignant tumours. Br J Surg 100:1764–1775
7. Abitabile P, Hartl U, Lange J, Maurer CA (2007) Radiofrequency ablation permits an effective treatment for colorectal liver metastasis. Eur J Surg Oncol 33:67–71
8. Martin RC, Scoggins CR, McMasters KM (2010) Safety and efficacy of microwave ablation of hepatic tumors: a prospective review of a 5-year experience. Ann Surg Oncol 17:171–178
9. Lu DS, Raman SS, Limanond P et al (2003) Influence of large peritumoral vessels on outcome of radiofrequency ablation of liver tumors. J Vasc Interv Radiol 14:1267–1274
10. Lu DS, Raman SS, Vodopich DJ, Wang M, Sayre J, Lassman C (2002) Effect of vessel size on creation of hepatic radiofrequency lesions in pigs: assessment of the "heat sink" effect. AJR Am J Roentgenol 178:47–51
11. Courivaud F, Kazaryan AM, Lund A et al (2014) Thermal fixation of swine liver tissue after magnetic resonance-guided high-intensity focused ultrasound ablation. Ultrasound Med Biol 40:1564–1577
12. Kim YS, Rhim H, Choi MJ, Lim HK, Choi D (2008) High-intensity focused ultrasound therapy: an overview for radiologists. Korean J Radiol 9:291–302
13. Holland GA, Mironov O, Aubry J-F, Hananel A, Duda JB (2013) High-intensity focused ultrasound. Ultrasound Clinics 8:213–226
14. Li S, Wu PH (2013) Magnetic resonance image-guided versus ultrasound-guided high-intensity focused ultrasound in the treatment of breast cancer. Chin J Cancer 32:441–452
15. de Senneville BD, Mougenot C, Quesson B, Dragonu I, Grenier N, Moonen CT (2007) MR thermometry for monitoring tumor ablation. Eur Radiol 17:2401–2410
16. Zhang L, Zhu H, Jin C et al (2009) High-intensity focused ultrasound (HIFU): effective and safe therapy for hepatocellular carcinoma adjacent to major hepatic veins. Eur Radiol 19:437–445
17. Jiang F, He M, Liu YJ, Wang ZB, Zhang L, Bai J (2013) High intensity focused ultrasound ablation of goat liver in vivo: pathologic changes of portal vein and the "heat-sink" effect. Ultrasonics 53:77–83
18. Kopelman D, Inbar Y, Hanannel A et al (2006) Magnetic resonance-guided focused ultrasound surgery (MRgFUS): ablation of liver tissue in a porcine model. Eur J Radiol 59:157–162
19. Sapareto SA, Dewey WC (1984) Thermal dose determination in cancer therapy. Int J Radiat Oncol Biol Phys 10:787–800
20. Chiang J, Willey BJ, Del Rio AM, Hinshaw JL, Lee FT, Brace CL (2014) Predictors of thrombosis in hepatic vasculature during microwave tumor ablation of an in vivo porcine model. J Vasc Interv Radiol 25:1965–1971 e1962
21. Chiang J, Cristescu M, Lee MH et al (2016) Effects of microwave ablation on arterial and venous vasculature after treatment of hepatocellular carcinoma. Radiology 281:617–624
22. Ishii T, Numata K, Hao Y et al (2017) Evaluation of hepatocellular carcinoma tumor vascularity using contrast-enhanced ultrasonography as a predictor for local recurrence following radiofrequency ablation. Eur J Radiol 89:234–241
23. Wijlemans JW, de Greef M, Schubert G et al (2015) A clinically feasible treatment protocol for magnetic resonance-guided high-intensity focused ultrasound ablation in the liver. Invest Radiol 50:24–31
24. Ramaekers P, de Greef M, van Breugel JM, Moonen CT, Ries M (2016) Increasing the HIFU ablation rate through an MRI-guided sonication strategy using shock waves: feasibility in the in vivo porcine liver. Phys Med Biol 61:1057–1077
25. Zhao LY, Liu S, Chen ZG, Zou JZ, Wu F (2016) Cavitation enhances coagulated size during pulsed high-intensity focussed ultrasound ablation in an isolated liver perfusion system. Int J Hyperthermia. https://doi.org/10.1080/02656736.2016.1255918:1-11
26. Ringe KI, Lutat C, Rieder C, Schenk A, Wacker F, Raatschen HJ (2015) Experimental evaluation of the heat sink effect in hepatic microwave ablation. PLoS One 10:e0134301
27. Chiang J, Hynes K, Brace CL (2012) Flow-dependent vascular heat transfer during microwave thermal ablation. Conf Proc IEEE Eng Med Biol Soc 2012:5582–5585
28. Wachsberg RH, Angyal EA, Klein KM, Kuo HR, Lambert WC (1997) Echogenicity of hepatic versus portal vein walls revisited with histologic correlation. J Ultrasound Med 16:807–810 quiz 811-802
29. Bangard C, Gossmann A, Kasper HU et al (2006) Experimental radiofrequency ablation near the portal and the hepatic veins in pigs: differences in efficacy of a monopolar ablation system. J Surg Res 135:113–119
30. Frericks BB, Ritz JP, Albrecht T et al (2008) Influence of intrahepatic vessels on volume and shape of percutaneous thermal ablation zones: in vivo evaluation in a porcine model. Invest Radiol 43:211–218